AIAA JOURNAL
Vol. 34, No. 7, July 1996

Technical Notes

TECHNICAL NOTES are short manuscripts describing new developments or important results of a preliminary nature. These Notes cannot exceed 6 manuscript pages and 3 figures; a page of text may be substituted for a figure and vice versa. After informal review by the editors, they may be published within a few months of the date of receipt. Style requirements are the same as for regular contributions (see inside back cover).

Viscoelastic Analysis of Thick-Walled Filament-Wound Composite Cylinders with Elevated Temperatures

Jerome T. Tzeng* and Larry S. Chien†
U.S. Army Research Laboratory,
Aberdeen Proving Ground, Maryland 21005

I. Introduction

TO date, activities in the research of viscoelasticity have mainly concerned isotropic materials, including the studies by Biot,[1] Muki and Sternberg,[2] Schapery,[3] Williams,[4] and Christensen.[5] These basic theories of viscoelasticity were then extended to the area of heterogeneous and anisotropic materials for a variety of applications. Hashin[6] used the effective relaxation moduli and creep compliances to define the macroscopic viscoelastic behavior of linear viscoelastic heterogeneous media and its implementation in viscoelastic modeling. The general formulation of linear viscoelastic boundary value problems of composite materials, including the thermal viscoelastic problems for thermorheologically simple materials and the applications of the correspondence principle, were examined by Schapery.[7] Rogers and Lee[8] investigated the viscoelastic behavior of an isotropic cylinder.

In the following research, the linear quasistatic viscoelastic behavior of a thick laminated composite cylinder with an elevated temperature change is studied. The analysis accounts for ply-by-ply variation of properties, temperature changes, and fiber orientations. The thick cylinder is assumed to be in the absence of thermomechanical coupling and to be in the state of generalized plane strain such that all of the stress and strain components are independent of the axial coordinate.[9,10] Moreover, because of the nature of axisymmetry, all of the stress and strain components are also independent of the circumferential coordinate. The mechanical responses of this thick composite cylinder will, therefore, only have to satisfy the governing equation in the radial direction. Invoking the Boltzmann superposition integral for the complete spectrum of increments of anisotropic material constants with respect to time, the thermoviscoelastic constitutive relations of the anisotropic composite cylinder can be derived in integral forms. Because the thick composite cylinder is subjected to a constant elevated temperature change and boundary conditions are all independent of time, formulations of the linear thermal viscoelastic problem can have forms identical to those of the corresponding linear thermoelastic problem by taking advantage of the elastic-viscoelastic correspondence principle. In other words, all of these integral constitutive equations reduce to the algebraic relations, which are very similar to those developed for thermoelastic media when they are Laplace transformed by means of the rule for convolution integrals. The thermoelastic analysis can thus be used to derive the transformed thermal viscoelastic solutions in the frequency domain.

Received April 21, 1993; revision received June 1, 1995; accepted for publication Aug. 20, 1995.

*Research Engineer, Weapons Technology Directorate.
†Postdoctoral Fellow, Weapons Technology Directorate.

II. General Formulation in Laplace Space

Consider a filament-wound axisymmetric thick composite cylinder consisting of N layers with the axial coordinate z, the radial coordinate r, and the circumferential coordinate θ, as shown in Fig. 1. This composite cylinder has the inner radius a, the outer radius b, and the length L. The Boltzmann superposition integral of stress σ_{ij} $(i, j = 1, 2, 3)$ and strain ϵ_{ij} $(i, j = 1, 2, 3)$ relation for an isothermal viscoelastic problem with a constant temperature increase ΔT and the thermal expansion coefficient α_{kl} is

$$\sigma_{ij}(t) = \int_0^t C_{ij}^{kl}(T, t-\tau)\frac{\partial \epsilon_{kl}(\tau)}{\partial \tau}\,d\tau - \beta_{ij}(T, t)\Delta T \qquad (1)$$

where $C_{ij}^{kl}(T, t)$ is the relaxation modulus dependent on temperature T and time t,

$$C_{ij}^{kl}[T(t), t] = C_{ij}^{kl}[T_0, \lambda(t)] \qquad \lambda(t) = \frac{t}{a_T[T(t)]}$$

Here, T_0 is the base temperature, and a_T is the temperature shift factor. The value $\beta_{ij}(T, t)$ is given by $B_{ij}(T, t) = C_{ij}^{kl}(T, t) \times \alpha_{kl}$. It is often desirable to use the inverse form of the constitutive relation (1),

$$\epsilon_{ij}(t) = \int_0^t A_{ij}^{kl}(T, t-\tau)\frac{\partial \sigma_{kl}(\tau)}{\partial \tau}\,d\tau + \psi_{ij}(T, t)\Delta T \qquad (2)$$

where $\psi_{ij}(T, t)$ is the tensor product of the creep compliance $A_{ij}^{kl}(T, t)$ and the thermal creep coefficient ϕ_{kl}. Because the elevated temperature change ΔT is constant above some reference value in time, the relaxation moduli and creep compliances are evaluated at that reference temperature regardless of whether or not the material is thermorheologically simple by employing the temperature shift factor.

The Laplace transform of a function $f(t)$ is defined as

$$\bar{f} = \bar{f}(s) = \int_0^\infty e^{-st} f(t)\,dt \qquad (3)$$

where s is the Laplace transform variable. Applying Eq. (3) with the convolution rule to Eqs. (1) and (2) reduces the integral constitutive equations to the following algebraic relations:

$$\bar{\sigma}_{ij} = \bar{C}_{ij}^{kl}\bar{\epsilon}_{kl} - \bar{\beta}_{ij}(\Delta T/s) \qquad (4)$$

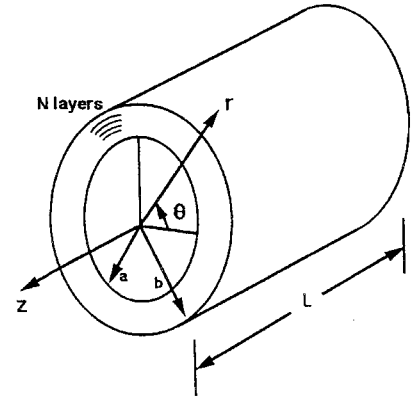

Fig. 1 Cylindrical coordinate system (r, θ, z) of an axisymmetric thick laminated composite cylinder containing N layers with the inner radius a, the outer radius b, and the length L.

and the inverse form

$$\bar{\epsilon}_{ij} = \tilde{A}_{ij}^{kl} + \tilde{\psi}_{ij}(\Delta T/s) \tag{5}$$

where

$$\tilde{C}_{ij}^{kl} = s\bar{C}_{ij}^{kl}, \qquad \tilde{A}_{ij}^{kl} = s\bar{A}_{ij}^{kl}, \qquad \tilde{\alpha}_{ij} = s\bar{\alpha}_{ij}$$

$$\tilde{\phi}_{ij} = s\bar{\phi}_{ij}, \qquad \tilde{\beta}_{kl} = \tilde{C}_{ij}^{kl} \cdot \tilde{\alpha}_{ij}, \qquad \tilde{\psi}_{kl} = \tilde{A}_{ij}^{kl} \cdot \tilde{\phi}_{ij}$$

Furthermore, it can be shown that $[\tilde{A}_{ij}^{kl}] = [\tilde{C}_{ij}^{kl}]^{-1}$.

Consider a corresponding thermoelastic problem with the transformed displacement components $\bar{u}$, $\bar{v}$, and $\bar{w}$ in the axial direction, the circumferential direction, and the radial direction, respectively, in each layer. The axisymmetric character of the thick composite cylinder along with the assumption of the state of generalized plane strain leads to a simplified displacement field, which reflects the circumferential independency and only radial dependency of $\bar{w}$,

$$\begin{aligned} \bar{u}(r, \theta, z) &= \bar{u}(r, z) \\ \bar{v}(r, \theta, z) &= \bar{v}(r, z) \\ \bar{w}(r, \theta, z) &= \bar{w}(r) \end{aligned} \tag{6}$$

Substituting these transformed displacement components into the strain-displacement relations and invoking the compatibility conditions, one can derive explicit forms of $\bar{u}$ and $\bar{v}$. Because each layer of the thick laminated cylinder is cylindrically monoclinic in reference to the global coordinates, there is no coupling between transverse shears and other deformations. Accordingly, the vanishing shear traction boundary conditions and interface continuity conditions generate zero out-of-plane shear tractions and shear strains for each layer. Moreover, owing to the absence of torsional deformation, the transformed displacement components $\bar{u}$ and $\bar{v}$ become

$$\bar{u} = \bar{\epsilon}^0 z \qquad \bar{v} = 0 \tag{7}$$

where the constant quantity $\bar{\epsilon}^0$ has the physical interpretation of transformed axial strain of a layer. In fact, $\bar{\epsilon}^0$, according to the present formulation, also represents the transformed axial strain of the entire composite cylinder. The calculation of $\bar{\epsilon}^0$ requires the knowledge of end boundary conditions and will be given later. Likewise, solving for $\bar{w}(r)$ requires the information of transformed strain components, the constitutive equations, as well as the equilibrium equations.

The earlier transformed displacement field gives the transformed strain components in cylindrical coordinates

$$\begin{aligned} \bar{\epsilon}_{rr} &= \frac{\mathrm{d}\bar{w}(r)}{\mathrm{d}r} \qquad & \bar{\epsilon}_{\theta\theta} &= \frac{\bar{w}(r)}{r} \\ \bar{\epsilon}_{zz} &= \frac{\mathrm{d}\bar{u}}{\mathrm{d}z} = \bar{\epsilon}^0 \qquad & \bar{\epsilon}_{\theta r} &= \bar{\epsilon}_{zr} = \bar{\epsilon}_z = 0 \end{aligned} \tag{8}$$

The unabridged form of the constitutive equation (4) for each layer in cylindrical coordinates with the radial coordinate r normal to the plane of symmetry is expressed as

$$\begin{Bmatrix} \bar{\sigma}_{zz} \\ \bar{\sigma}_{\theta\theta} \\ \bar{\sigma}_{rr} \\ \bar{\sigma}_{\theta r} \\ \bar{\sigma}_{zr} \\ \bar{\sigma}_{z\theta} \end{Bmatrix} = \begin{Bmatrix} \tilde{C}_{11} & \tilde{C}_{12} & \tilde{C}_{13} & 0 & 0 & \tilde{C}_{16} \\ \tilde{C}_{12} & \tilde{C}_{22} & \tilde{C}_{23} & 0 & 0 & \tilde{C}_{26} \\ \tilde{C}_{13} & \tilde{C}_{23} & \tilde{C}_{33} & 0 & 0 & \tilde{C}_{36} \\ 0 & 0 & 0 & \tilde{C}_{44} & \tilde{C}_{45} & 0 \\ 0 & 0 & 0 & \tilde{C}_{45} & \tilde{C}_{55} & 0 \\ \tilde{C}_{16} & \tilde{C}_{26} & \tilde{C}_{36} & 0 & 0 & \tilde{C}_{66} \end{Bmatrix} \times \begin{Bmatrix} \bar{\epsilon}_{zz} \\ \bar{\epsilon}_{\theta\theta} \\ \bar{\epsilon}_{rr} \\ \bar{\epsilon}_{\theta r} \\ \bar{\epsilon}_{zr} \\ \bar{\epsilon}_{z\theta} \end{Bmatrix} - \frac{\Delta T}{s} \begin{Bmatrix} \tilde{B}_{zz} \\ \tilde{B}_{\theta\theta} \\ \tilde{B}_{rr} \\ 0 \\ 0 \\ \tilde{B}_{z\theta} \end{Bmatrix} \tag{9}$$

Furthermore, from the preceding discussions, it can be shown that two of the three equilibrium equations are satisfied automatically. The only nontrivial equilibrium equation is the one in the radial direction,

$$\frac{\partial \bar{\sigma}_{rr}}{\partial r} + \frac{\bar{\sigma}_{rr} - \bar{\sigma}_{\theta\theta}}{r} = 0 \tag{10}$$

Substituting Eqs. (6–8) into Eq. (9), the transformed stress components $\bar{\sigma}_{rr}$ and $\bar{\sigma}_{\theta\theta}$ are obtained in terms of the transformed radial displacement $\bar{w}$. Incorporating the resulting $\bar{\sigma}_{rr}$ and $\bar{\sigma}_{\theta\theta}$ functions with Eq. (10) gives a nonhomogeneous Euler differential equation of $\bar{w}$ for a layer

$$r^2 \frac{\mathrm{d}^2\bar{w}}{\mathrm{d}r^2} + r\frac{\mathrm{d}\bar{w}}{\mathrm{d}r} - \tilde{\lambda}^2\bar{w} = \frac{r}{\tilde{C}_{33}}\left[\frac{\Delta T}{s}(\tilde{B}_{rr} - \tilde{B}_{\theta\theta}) - (\tilde{C}_{13} - \tilde{C}_{12})\bar{\epsilon}^o\right] \tag{11}$$

where

$$\tilde{\lambda}^2 = \tilde{C}_{22}/\tilde{C}_{33} \tag{12}$$

Solving Eq. (11) for $\bar{w}$ yields

$$\bar{w} = \bar{A}_1 r^{\tilde{\lambda}} + \bar{A}_2 r^{-\tilde{\lambda}} + \bar{w}_p \tag{13}$$

where

$$\begin{aligned} \bar{w}_p &= \tilde{f}_1 \bar{\epsilon}^o r + \tilde{f}_3 r \\ \tilde{f}_1 &= \frac{\tilde{C}_{12} - \tilde{C}_{13}}{\tilde{C}_{33} - \tilde{C}_{22}} \\ \tilde{f}_3 &= \frac{\tilde{S}}{\tilde{C}_{33} - \tilde{C}_{22}} \\ \tilde{S} &= (\Delta T/s)[\tilde{B}_{rr} - \tilde{B}_{\theta\theta}] \end{aligned} \tag{14}$$

and $\bar{A}_1$ and $\bar{A}_2$ are coefficients to be determined from boundary and continuity conditions.

Finally, it is understood that the initial condition of the original thermoviscoelastic problem is displacement-free state of rest. The boundary conditions are of free tractions and, hence, of free transformed tractions on both inner and outer circular surfaces,

$$\bar{\sigma}_{rr} = \bar{\sigma}_{\theta r} = \bar{\sigma}_{zr} = 0 \qquad \text{at} \qquad r = a, b \tag{15}$$

On both end surfaces, stress resultants are zero:

$$\sum_{k=1}^{N} \int_{r_i}^{r_o} \bar{\sigma}_{zz} r \, \mathrm{d}r = \bar{\sigma}_{zr} = \bar{\sigma}_{z\theta} = 0 \qquad \text{at} \qquad z = 0, L \tag{16}$$

where r_i and r_o are inner and outer radii, respectively, of the kth layer. The continuity conditions at each interface between two adjacent layers require continuous radial traction and continuous radial displacement at any instant as shown in Fig. 2. Thus, when written in the transformed form, they become

$$\bar{\sigma}_{rr,o}^{(k)} - \bar{\sigma}_{rr,i}^{(k+1)} = 0 \tag{17}$$

and

$$\bar{w}_{,o}^{(k)} = \bar{w}_{,i}^{(k+1)} \tag{18}$$

where $k = 1, \ldots, N-1$, and subscripts i and o denote inner and outer surfaces, respectively.

III. Results and Discussion

The time-dependent thermal viscoelastic behavior of a 100-layer AS-4/3502 graphite epoxy composite cylinder subjected to a temperature increase $\Delta T = 150°C$ is examined. The composite cylinder has an inner radius $a = 3.5$ in., an outer radius $b = 4.1$ in., and a thickness of each layer $h = 6.0 \times 10^{-3}$ in. Stacking sequence is given as $[0/30/60/90]_{2S}$ from inside out with the 0-deg direction coinciding with the axis of the cylinder. The creep properties of AS-4/3502 graphite epoxy and AS-4/PEEK thermoplastic laminate with a fiber volume fraction of 0.67 were investigated at different temperatures by Kim and Hartness.[11] In this study, the least-squares curve fitting was used to express the creep compliances from the original AS-4/3502 data at $T = 150°C$ in a power law form

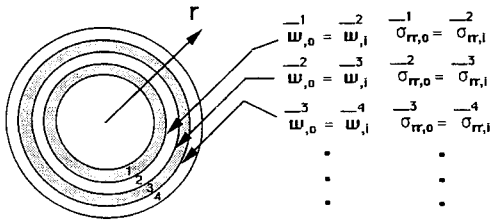

Fig. 2 Normal traction continuity and normal displacement continuity at the interfaces between two adjacent layers with the radial displacement $\bar{w}$, the outside surface o, the radial stress $\bar{\sigma}_{rr}$, and the inside surface i.

$$S_{22}(t) = [1.7051(t)^{0.1954} + 1]S_{22}^0 \tag{19}$$

and

$$S_{66}(t) = [11.3076(t)^{0.2771} + 1]S_{66}^0 \tag{20}$$

where

$$S_{22}^0 = 7.5328 \times 10^{-7}/\text{psi} \qquad S_{66}^0 = 1.3834 \times 10^{-6}/\text{psi}$$

The compliance in the fiber direction, $S_{11} = 5.9 \times 10^{-8}$/psi, and Poisson's ratios, $\nu_{12} = \nu_{13} = 0.3$ and $\nu_{23} = 0.36$, are assumed to be

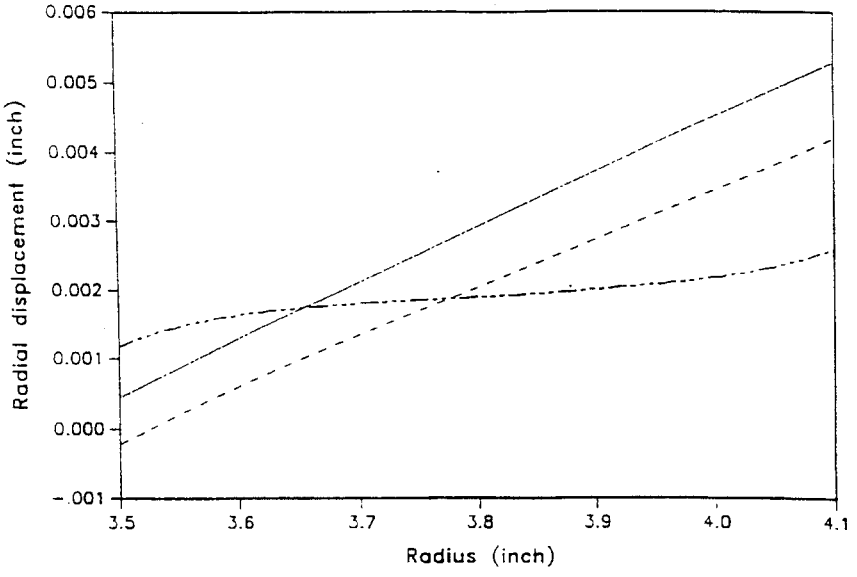

Fig. 3 Radial displacement profiles across the thickness of the cylinder at three different instants: · — ·, $t = 10^{-3}$ min; - - -, $t = 10^{4.5}$ min; and — - -, $t = 10^{12}$ min.

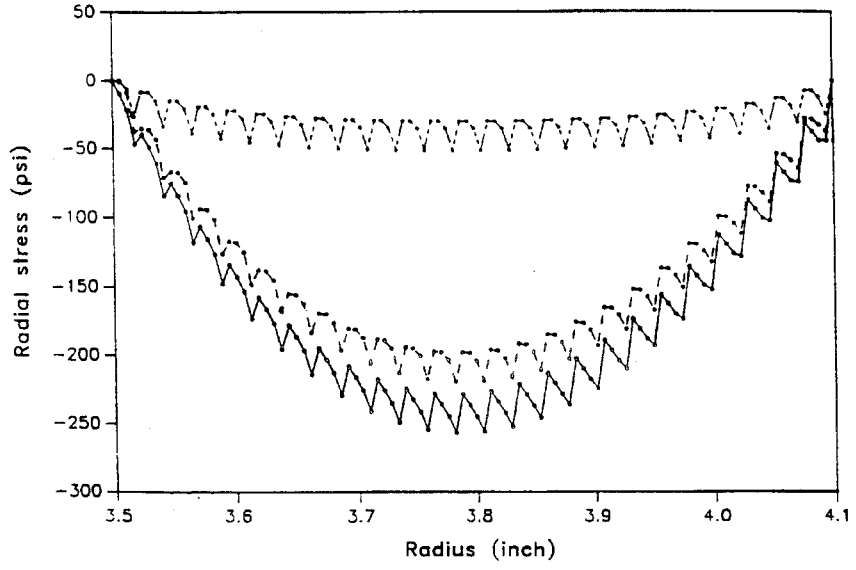

Fig. 4 Radial stress profiles across the thickness of the cylinder at three different instants: —●—, $t = 10^{-3}$ min; -●-, $t = 10^{4.5}$ min; and — - -, $t = 10^{12}$ min.

time independent. Thermal expansion coefficients of the composites in three principal directions are $\alpha_{11} = -0.5 \times 10^{-6}/°C$ and $\alpha_{22} = \alpha_{33} = 40.0 \times 10^{-6}/°C$, where the negative value indicates shrinkage with temperature increase.

Figures 3 and 4 show radial displacement and radial stress profiles across the thickness of the cylinder at three instants, $t = 10^{-3}$ min, $t = 10^{4.5}$ min, and $t = 10^{12}$ min, respectively. The radial tractions and displacements satisfied the continuity conditions at the interfaces of layers at all instants. The saw-shaped radial stress distribution is resulted from the discontinuity of material properties and various fiber orientations. The radial displacement $w(t)$ reaches a steady state at $T = 10^{12}$ min due to a long-term creep behavior. The radial displacement of most layers reaches a constant value, except at the innermost and outermost portions of the cylinder. The free traction boundary at the surface of cylinders causes the gradients in the radial displacements. A similar phenomenon is also observed in the radial stresses showing a constant level of stress distribution in the inner portion of cylinder away from boundary layers at $t = 10^{12}$ min. This long-term creep characteristic reflects the proposed power law form, Eqs. (19) and (20), of the creep compliances.

IV. Conclusions

An analysis was developed to study the thermal viscoelastic behavior of thick-walled laminated composite cylinders. The formulation accounts for ply-by-ply variations of material properties and temperature changes. The matrix form numerical solution with parallel computing techniques resolved the complexity and time-consuming calculation procedures in the Laplace transform of a multilayered composite cylinder. The creep behavior of materials and relaxation of thermal stresses in a cylinder subjected to a uniform temperature change were properly predicted illustrating the capability of the analysis. Because the viscoelastic properties exist only in matrix dominant properties, such as transverse and shear properties, the viscoelastic behavior of anisotropic laminated cylinders is quite different from those of isotropic cylinders. The stresses will not diminish due to elastic properties in the fiber direction. The developed analysis will be very useful to study the viscoelastic behavior of cylinders under thermal loads and thermal residual stresses due to the manufacturing processes of thermoplastic composites.

References

[1]Biot, M. A., "Linear Thermodynamics and the Mechanics of Solids," *Proceedings, 3rd U.S. National Congress of Applied Mechanics*, American Society of Mechanical Engineers, New York, 1958, pp. 1–18.

[2]Muki, R., and Sternberg, E., "On Transient Thermal Stresses in Viscoelastic Materials with Temperature Dependent Properties," *Journal of Applied Mechanics*, Vol. 28, Series E, No. 2, 1961, pp. 193–207.

[3]Schapery, R. A., "Application of Thermodynamics to Thermomechanical, Fracture, and Birefringent Phenomena in Viscoelastic Media," *Journal of Applied Physics*, Vol. 35, No. 5, 1964, pp. 1451–1465.

[4]Williams, M. L., "Structural Analysis of Viscoelastic Materials," *AIAA Journal*, Vol. 2, No. 5, 1964, pp. 785–808.

[5]Christensen, R. M., *Theory of Viscoelasticity, An Introduction*, 2nd ed., Academic, New York, 1982.

[6]Hashin, Z., "Viscoelastic Behavior of Heterogeneous Media," *Journal of Applied Mechanics*, Vol. 32, Series E, No. 3, 1965, pp. 630–636.

[7]Schapery, R. A., "Stress Analysis of Viscoelastic Composite Materials," *Journal of Composite Materials*, Vol. 1, No. 3, 1967, pp. 228–267.

[8]Rogers, T. G., and Lee, E. H., "The Cylinder Problem in Viscoelastic Stress Analysis," *Quarterly of Applied Mathematics*, Vol. 22, No. 2, 1964, pp. 117–131.

[9]Tzeng, J. T., and Chien, L. S., "A Thermal/Mechanical Model of Axially Loaded Thick-Walled Composite Cylinders," *Journal of Composites Engineering*, Vol. 4, No. 2, 1994, pp. 219–232.

[10]Chien, L. S., and Tzeng, J. T., "A Thermal Viscoelastic Analysis for Thick-Walled Composite Cylinders," *Journal of Composite Materials*, Vol. 29, No. 4, 1995, pp. 525–548.

[11]Kim, R. Y., and Hartness, J. T., "Time-Dependent Response of AS-4/PEEK Composite," *Proceedings of the 19th International SAMPE Technical Conference*, Society for the Advancement of Material and Process Engineering, Covina, CA, 1987, pp. 468–475.

Correlation of Shock Angles Caused by Rhombic Delta Wings

S. Koide,*C. J. W. Griesel,† and J. L. Stollery‡
Cranfield University,
Bedford, England, United Kingdom

Introduction

In the past five years, the authors have investigated the effects of strakes on the glancing shock-wave/turbulent-boundary-layer interaction generated by an unswept sharp fin placed on a wall (see Fig. 1).[1,2] To consider the role of the shock structure on the interaction behavior, the inviscid flowfields around the fin with one of several different strakes were calculated by an Euler computational fluid dynamics (CFD) solver. Figure 1 shows a three-dimensional inviscid-shock structure deduced from the computed flowfields. The shock structure consists of two shock waves, one from the strake and the other from the unmodified part of the fin, and they are expressed by strake shock and fin shock, respectively, in Fig. 1. To consider the roles of the shocks, traces of the two shock waves on the wall provided important reference positions (the imaginary positions that would exist if no boundary layer were presented on the wall). But no simple solutions existed to predict these positions. In this Note, flowfields around a series of rhombic delta wings (RDWs; see Fig. 2) are calculated by the Euler CFD solver to predict the strake shock location on the wall. This is because the RDWs generate inviscid shock waves appropriate to the strake shock. Using the computed data, a correlation law with Mach number M and wing geometry is constructed for predicting the shock angle in the plane of symmetry of the wing β (see Fig. 2, corresponding to the strake-shock angle on the wall of Fig. 1). Once the shock angle is predicted using the correlation law, the strake-shock trace can be specified on the wall as long as the shock remains attached to the strake apex. As to the fin-shock location, a prediction method has been proposed in Refs. 1 and 2.

Computation Method

An Euler CFD code developed by Griesel[3] was employed for the present configurations. In Griesel's solver, a Riemann-problem-based, shock-capturing method was applied to the solution of the steady Euler equations. The code has already been well validated using two-dimensional models such as a wedge in a duct, a backward-facing ramp, and a biconvex airfoil.[3] In addition, the computed shock angles β for a rhombic delta wing (see Fig. 2) were compared with experimental angles obtained by schlieren photography. They were in excellent agreement for wing half-apex angles α ranging from 8 to 14 deg and for wing sweep angles λ of 45 and 60 deg at $M = 2.45$.[1]

Correlation of the Shock Angles

To collect data for constructing a correlation law of the shock angle β with M and the wing geometry (as specified by α and λ, see Fig. 2), flowfields around a series of RDWs were calculated by the Euler CFD solver. The CFD calculations were carried out for RDWs with $30 \leqq \lambda \leqq 60$ deg and $8 \leqq \alpha \leqq 17$ deg ($\leqq 14$ deg at $M = 2.0$) at $M = 2.0$, 2.46, and 3.5. This range was chosen to include the experimental condition of Refs. 1 and 2, together with a wider band of supersonic Mach numbers under which the shock wave remains attached to the delta wing apex. Figure 2 shows an example of the computed pressure field in the plane of symmetry. The solid circles

Received April 19, 1995; revision received Aug. 11, 1995; accepted for publication Aug. 11, 1995.

*Ph.D. Student, College of Aeronautics; currently Senior Research Engineer, 2-5th Lab., 3rd Research Centre, Japan Defense Agency, 1-2-10 Sakae, Tachikawa, Tokyo 190, Japan. Member AIAA.

†Ph.D. Student, College of Aeronautics. Student Member AIAA.

‡Professor, Head of College of Aeronautics. Fellow AIAA.